The ROS scavenging and renal protective effects of pH-responsive nitroxide radical-containing nanoparticles

Toru Yoshitomi[a], Aki Hirayama[b] and Yukio Nagasaki[a,c,d,*]

[a] Graduate School of Pure and Applied Sciences, University of Tsukuba, Tennoudai 1-1-1, Tsukuba, Ibaraki, 305-8573, Japan

[b] Center for Integrative Medicine, Tsukuba University of Technology, Kasuga 4-12-7, Tsukuba, 305-8521, Ibaraki, Japan

[c] Master's School of Medical Sciences, Graduate School of Comprehensive Human Sciences, University of Tsukuba, Tennoudai 1-1-1, Tsukuba, Ibaraki, 305-8573, Japan

[d] Satellite Laboratory, International Center for Materials Nanoarchitectonics (MANA), National Institute for Materials Science (NIMS), Tennoudai 1-1-1, Tsukuba, Ibaraki, 305-8573, Japan

[*]Corresponding author: Prof. Yukio Nagasaki, Graduate School of Pure and Applied Sciences, Master's School of Medical Sciences, Graduate School of Comprehensive

Human Sciences, Satellite Laboratory, International Center for Materials Nanoarchitectonics (MANA), National Institute for Materials Science (NIMS), University of Tsukuba, Tennoudai 1-1-1, Tsukuba, Ibaraki, 305-8573, Japan

Phone: +81-29-853-5749

Fax: +81-29-853-5749

E-mail information: yukio@nagalabo.jp

Abstract

The ultimate objective of nanoparticle-based therapy is to functionalize nanomedicines in a micro-disease environment without any side effects. Here, we reveal that our pH-responsive nitroxide radical-containing nanoparticles (RNP^{pH}) disintegrate within the renal acidic lesion and act as scavengers of reactive oxygen species (ROS), leading to a relief of acute kidney injury (AKI). RNP^{pH} was prepared using amphiphilic block copolymers possessing 2,2,6,6-tetramethylpiperidine-*N*-oxyl (TEMPO) moieties via amine linkage as a side chain of the hydrophobic segment. The self-assembled RNP^{pH} disintegrated at pH below 7.0 because of a protonation of the amino groups in the hydrophobic core of the nanoparticles, thereby resulting in an improvement in ROS scavenging activity. Using a renal ischemia-reperfusion AKI model in mice, the therapeutic effect of RNP^{pH} on ROS damage was evaluated. Unlike the RNP without pH-triggered disintegration (RNP^{Non-pH}), the RNP^{pH} showed extremely high ROS scavenging activity and renal protective effects. It is interesting to note that the side effect of nitroxide radicals was markedly suppressed due to the compartmentalization of nitroxide radicals in the core of RNP^{pH} in untargeted area. The morphology changes in RNP^{pH} were confirmed by analyzing electron spin resonance spectra, and these findings provide the evidence of the real therapeutic effect

of the environment-sensitive specific disintegration of nanoparticles in vivo.

Introduction

Acute kidney injury (AKI) is evoked by multiple disorder and the morbidity and mortality rates of AKI patients have been keeping high level despite significant advances in the management of the disease in recent years [1]. One potential mechanism for the irreversible damage is the generation of reactive oxygen species (ROS), which leads to the stimulation of pro-apoptotic mediators, inflammatory cytokines and further oxidative stress [2 - 4]. Redox-targeted therapies using antioxidants have been attracted much attention and widely attempted clinically. Though they worked to some extent, it remains incomplete [5]. Since redox reaction is one of the most important events in biological activity, severe and unexpected side effects were caused if antioxidant turns around the body after high-dose administration. To obtain therapeutic efficiency and suppress unwanted effects, the innovative strategy must be required. If drug, which effectively scavenges ROS excessively generated at specific-lesion, retaining dormant character under untargeted area, it can be safe and effective medication.

To improve the therapeutic efficiencies of drugs, the precise control of pharmacokinetics is crucial. Drug delivery nanoparticles using polymeric micelles or liposomes are able to control the drug pharmacokinetics and some of them have already

been commercialized for anti-cancer therapy [6-8]. Nanoparticles are known to

accumulate in specific regions because of the changes in the specific vascular

microenvironment [9]. More than 90 % of the nanoparticles, however, spread

non-specifically in vivo after systemic administration [10,11]. Active targeting is one

of the challenges to improve nanoparticle accumulation in specific disease areas;

however, to date, no remarkable effect on its biodistribution has been reported [12].

When ligands with high specificity are installed on the carrier surface, its blood

circulation tendency often decreases due to the lowered colloidal stability [13]. Even

if the ligand-installed carrier works well in vitro, it is very difficult to effectively work

under in vivo conditions. One promising target to improve the efficiency of

nanotherapy is "on-off regulation", whereby the nanoparticle is dormant in non-target

tissue and is activated in the target area, thus improving treatment outcomes and

decreasing side effects [14].

Here, we propose a promising therapy, "Environmental-Signal-Enhanced Polymer

Drug Therapy" (ESEPT) for AKI (see Fig. 1). The main concepts of ESEPT are: (1)

installation of the drug in a hydrophobic segment of an amphiphilic block copolymer

via a covalent linkage; (2) self-assembly of the block copolymer to compartmentalize

the drugs in the core of the nanoparticle; and (3) disintegration of the nanoparticle in

response to a signal, such as pH, in the disease environment. Thus, the ESEPT strategy improves the therapeutic efficiency and suppresses the significant side effects. The polymer designed for ESEPT in this study is a poly(ethylene glycol)-b-poly(methylstyrene) (PEG-b-PMS) block copolymer, attached to 2,2,6,6-tetramethylpiperidine-N-oxyl (TEMPO) via an amine linkage (PEG-b-PMNT) (see Fig. 1) [15]. PEG-b-PMNT forms a core-shell type of self-assembling polymeric micelle in aqueous media, and it disintegrates under acidic conditions due to the protonation of amino groups located in the core of the nitroxide-radical-containing particle (RNP^{pH}) [16,17]. Simultaneously, the RNP^{pH} exposes the nitroxide radicals, which can catalytically scavenge ROS [18,19]. Therefore, we hypothesized that the treatment of AKI is a suitable target of ESEPT by RNP^{pH}. The aim of this study was to demonstrate a rational strategy for ESEPT using a renal ischemia-reperfusion (IR) induced AKI model in mice. If RNP^{pH} can disintegrate and scavenge ROS in response to low pH in renal ischemic regions [20], it might become an ideal therapeutic nanoparticle for AKI.

Methods

Preparation of RNP^{pH}

pH-responsive RNP^{pH} was prepared by a self-assembling PEG-*b*-PMNT block copolymers, as previously reported [15,16]. Briefly, MeO-PEG-*b*-poly(chloromethylstyrene) (PCMS) was synthesized by the radical telomerization of chloromethylstyrene (CMS) using MeO-PEG-SH (Mn = 5,000) as a telogen. To obtain PEG-*b*-PMNT, the chloromethyl groups on the PCMS segment of the block copolymer were converted to nitroxide radicals via the amination of MeO-PEG-*b*-PCMS with 4-amino-TEMPO in DMSO. The RNP^{pH} was prepared from MeO-PEG-*b*-PMNT by the dialysis method. Final concentration of RNP^{pH} was adjusted by PBS. Please see Supplementary Methods about dialysis method.

Preparation of RNP^{Non-pH}

Non-pH-responsive RNP^{Non-pH} was prepared by a self-assembling amphiphilic block copolymer (PEG-*b*-PMOT) composed of the PEG segment and the PMS segment possessing TEMPO moieties as a side chain via ether linkage, as show in Fig. S1. Please see Supplementary Methods about detailed preparation method.

Measurement of the scavenging activity of RNP against superoxide

The spin trap method was performed using 5,5-dimethyl-1-pyrroline-N-oxide (DMPO) as a spin-trapping agent to detect superoxide generated by the reaction of

xanthine with xanthine oxidase (XOD).   Briefly, 5 μL of 10 U/mL XOD solution were added to the mixture of xanthine solution (5 μL**,** 20 mM), DMPO solution (10 μL, 1 mM) in milliQ water containing diethylenediaminepentaacetate (0.1 mM) and Britton-Robinson buffer (70 μL) (pH 6.0 and pH 7.4) prepared from a stock solution containing 1 M phosphoric acid, 1 M boric acid and 1 M acetic acid, and by adjusting the pH value with NaOH in the presence or absence of RNP solution (10 μL) (nitroxide concentration: 3.3 μM).   The mixture was immediately transferred to a capillary tube, followed by measurement of the ESR spectrum.   The final concentrations of the DMPO, xanthine, XOD, and TEMPO radicals in RNP were 100 μM, 1 mM, 0.5 U/mL and 0.33 μM, respectively.   Because the ESR spectra of DMPO overlap with ESR spectra of RNP, signal intensities of DMPO were subtracted from the RNP spectra (see Supplementary Fig. S2).

Animals

Male ICR mice between 9 and 11 weeks old were maintained in the experimental animal facilities at the University of Tsukuba.   All experiments were performed according to the Guide for the Care and Use of Laboratory Animals at the University of Tsukuba.

Renal ischemia-reperfusion

Animals were anesthetized initially with pentobarbital sodium (40 mg/kg). After right heminephrectomy, the left renal pedicle was clamped through flank incisions for 50 min using a microvascular clip to produce ischemia and then reperfusion was performed. In addition, another group of mice was subjected to flank incision and right heminephrectomy as the sham-operated control group. The animals were randomly divided to receive intravenous injection of RNP^{pH} (3 mg/kg), RNP^{Non-pH} (1.5 mg/kg), 4-hydroxyl-TEMPO (0.4 mg/kg), 4-amino-TEMPO (0.4 mg/kg), and vehicle (PBS) at 5 min after reperfusion.

Assessment of renal function

Blood samples were collected by intracardiac puncture using heparined syringe at 24 h after reperfusion. Then, plasma samples were obtained by centrifugation (6,200 rpm, 2000 g, 10 min) of the blood. Plasma samples were assayed for BUN and Cr using a Fuji Dri-chem 3500 (Fuji-Film, Tokyo, Japan).

Morphological studies

Please see Supplementary Methods.

Measurement of renal superoxide production

To determine superoxide production, kidneys excised from mice were homogenized in sucrose buffer (0.32 M sucrose, 10 mM Tris-HCl, pH 7.4) on ice with a homogenizer. The kidney lysate (100 μL) was moved to a 96-well black plate (NUNC) containing 3.3 mM dihydroethidium (DHE; Wako), followed by incubation at 37 ºC for 20 min. The fluorescent intensity of each well was measured at a spectrum wavelength of excitation at 530 nm and emission at 620 nm. DHE alone was read to calculate a zero-point. Superoxide values, which subtracted the zero-point value, were expressed as intensity per 100 μg of protein. To determine superoxide production histologically, kidneys excised from mice were embedded in Tissue-Tek oxytetracycline (OTC) compound (Funakoshi, Japan) on the dry ice. Later, the tissue samples were sliced into 20-μm cryo-sections using a cryotome (Leica). The cryo-sections were then washed in PBS and stained with 1 mM DHE to detect superoxide formation. The sections were incubated for 30 min with DHE solution at room temperature, mounted with Prolong Gold anti-fade reagent (Invitrogen), and observed under a microscope (Leica).

Cytokine measurements

Plasma levels of cytokines were determined at 24 h after reperfusion. IL-6 was measured by a commercial available enzyme-linked immunoassay kit (Thermo Scientific Pierce Protein Research Products) according to manufacturer's instrument.

Measurement of TBARS

The degree of lipid peroxidation in the kidney tissue was determined by measuring the malondialdehyde (MDA) levels with TBARS. Kidney was frozen and stored at -80 ˚C until the assay. Briefly, a 10 % (wt/vol) kidney homogenate was prepared in 0.1 M PB solution containing 1 mM EDTA followed by centrifugation at 600 g for 15 min at 4 ˚C. An aliquot of the supernatant was added to the reaction mixture containing 8 % SDS, 20 % acetic acid, 0.8 % thiobarbituric acid, and water. After incubation at 95 ˚C for 1 h, the amount of MDA formed in the reaction mixture was measured by a spectrophotometer at an absorbance of 532 nm. MDA was used as the standard, and TBARS values were expressed as nmol per mg protein.

ESR Measurement of concentration of the nitroxide radicals in blood and in kidney.

ICR mice subjected to IR injury were anesthetized via an intraperitoneal injection of pentobarbital sodium (40 mg/kg). Following this, RNPs or low-molecular-weight TEMPO derivatives in PBS solution (nitroxide radical concentration: 75 mmol/kg, 350 μL) was injected intravenously. Blood samples were collected from the heart using a heparinized syringe at 0.083, 0.25, 0.5, 3, 6 and 24 h after the administration, and the kidney was excised immediately after blood collection. The blood and kidney were immediately placed on ice. Plasma samples were then obtained by centrifuging (6,200 rpm, 2000 g, 10 min) the blood samples. It was confirmed that no ESR signal was observed in the blood cell precipitates after centrifugation. The ESR signal intensities in these plasma samples were measured by X-band ESR spectrometer (JES-TE25X; JEOL, Tokyo, Japan) at room temperature. In the case of the ESR intensities at 0 min, 12.5 μL of RNP solution (0.9 mg/mL) was added to the blood (100 μL), followed by centrifugation (6,200 rpm, 2000 g, 10 min) of the blood and ESR measurement, assuming that the total blood volume in mice is 80 mL/kg. The kidney tissue homogenates were prepared by a homogenizer. The total amount of drug (nitroxide radicals + hydroxyamines) in blood and kidney were estimated from X-band ESR measurements of the sample after addition of $K_3[Fe(CN)_6]$, which was prepared at 200 mM as a stock solution. The ESR measurements were

13

carried out under the following conditions: frequency, 9.41 GHz; power, 8.00 mW; field,

333.8 ± 5 mT; sweep time, 1.0 min; modulation, 0.1 mT; time constant, 0.1 s.

Effect of RNP on blood pressure

Ten-weeks-old ICR mice were anesthetized with an interperitoneal injection of

pentobarbital sodium (40 mg/kg). Blood pressure was measured at 15 min after

intravenous administration of PBS, RNP^{pH}, RNP^{Non-pH}, amino-TEMPO or

hydroxyl-TEMPO by the indirect tail-cuff method with a blood pressure monitor (model

MK-1030, Muromachi Kikai, Tokyo, Japan).

Statistical analysis

All values are expressed as mean $\pm$ SE. Continuous data between groups were

compared by one-way ANOVA. All ANOVAs were performed with ANOVA tests

followed by Tukey's test. Differences with a value of $P < 0.05$ were considered

statistically significant.

Results

Characterization of RNP

      To test for the effectiveness of ESEPT, we prepared a nitroxide-radical-containing-particle without pH-triggered disintegration (RNP^{Non-pH}) as a comparative nanopariticle. Physicochemical characterization of both RNPs was carried out. The size of RNP^{pH} (average diameter, 46 nm; polydispersity factor, μ/Γ^2 = 0.035) was almost similar to that of RNP^{Non-pH} (average diameter, 42 nm; polydispersity factor, μ/Γ^2 = 0.061) (see Fig. 2a). Fig. 2b shows the scattering intensities of both RNPs as a function of pH. The light scattering intensity of RNP^{pH} drastically decreased at pH values below 7.0; in contrast, there was no change in the case of RNP^{Non-pH}. According to the Rayleigh approximation ($I \propto d^6$, where I is the scattering intensity and d is the particle size), it is clear that RNP^{pH} disintegrates at pH values below 7.0 and that RNP^{Non-pH} does not disintegrate in response to pH. To investigate the pH response of the superoxide scavenging activities of both RNPs, ROS spin-trapping experiments were carried out at pH 6.0 and 7.4. As shown in Fig. 2c, the ROS scavenging activity of RNP^{Non-pH} did not change at pH 6.0 and 7.4, whereas the activity of RNP^{pH} significantly increased in response to lowered pH. This result indicates that RNP^{pH} can expose nitroxide radicals from the RNP^{pH} core and effectively

15

scavenge superoxide anions due to the disintegration of RNP^{pH} in response to lowered pH.

Therapeutic effect of RNP on IR-AKI

To determine the therapeutic effect of RNP^{pH} on AKI, we prepared a renal IR model in mice.   Ischemic renal failure in ICR mice was initiated by right nephrectomy and clamping of the left renal artery and vein for 50 min.   A significant difference was observed in the values of blood urea nitrogen (BUN) and creatinine (Cr) (Supplementary Information, Fig. S3) between the sham-operated group (0 min IR) and 50-min IR group.   At 5 min after reperfusion, 350 μL of RNP^{pH} (3 mg/kg), RNP^{Non-pH} (1.5 mg/kg), 4-amino-TEMPO (0.4 mg/kg) or 4-hydroxy-TEMPO (0.4 mg/kg) was administered into the tail vein of mice (body weight: ca. 35 g) subjected to renal IR.   It should be noted that the concentrations of nitroxide radicals in all drugs were the same, which were adjusted by measurements of electron spin resonance (ESR) spectra (see Supplementary Information, Table S1).   None of drugs caused renal dysfunction or had any other toxicity in normal ICR mice (Supplementary Information, Fig. S4).   At 24 h after reperfusion, RNP^{pH} treated mice had BUN and Cr of 25.46 mg/dl and 0.31 mg/dl

versus 129.86 and 2.69 for vehicle, versus 30.27 and 0.43 for 4-hydroxy-TEMPO and

versus 48.23 and 0.74 for 4-amino-TEMPO (see Fig. 3a and 3b). Clearly, the RNP^{pH}

outperforms low-molecular-weight TEMPO derivatives in reducing renal dysfunction.

Moreover, therapeutic effect of RNP^{pH} was greater than that of RNP^{Non-pH} (BUN; 34.29,

Cr; 0.89), indicating that the disintegration of RNP^{pH} might improve its therapeutic

efficiency. To further investigate renal IR injury after treatment, hematoxylin and

eosin (HE) staining was conducted. As shown in Fig. 3c and Table 1, HE staining

revealed that tubular cell swelling, interstitial edema, and tubular dilatation were

significantly more severe in the vehicle-treated IR mice than the sham-operated mice.

Compared to other treatments, the treatment with RNP^{pH} resulted in significantly less

damage, similar to the measurements of BUN and Cr.

We also investigated whether RNP^{pH} could scavenge ROS, in particular

superoxide, generated in the injured kidney. As shown in Fig. 4a and 4b, the

generation of ROS in kidney was significantly inhibited by the treatment with RNP^{pH} in

comparison to other treatments. Additionally, we investigated whether RNPs can

inhibit lipid peroxidation and generation of the inflammation cytokine. Compared

with other treatments, treatment with RNP^{pH} resulted in a significant reduction of

thiobarbituric acid reactive substance (TBARS) levels, which serve as an index of lipid

peroxidation in kidney, and the generation of inflammation cytokine in plasma, as can be seen in Fig. 4c and 4d, respectively. In particular, TBARS level of RNP^{pH} treated group was statistically lower than that of other groups as shown in Fig. 4c. These results provide the reason of the high therapeutic efficiency of RNP^{pH}.

Conformational changes of the nanoparticle in the injured kidney

To demonstrate the reason that RNP^{pH} showed superior therapeutic effect on renal IR injury, we utilized the ESR measurement. Since nitroxide radicals in the RNP core are susceptible to ESR, the spectra can provide information on morphological changes in the RNP. Generally, the ESR signal of low-molecular-weight TEMPO derivatives shows a sharp triplet due to an interaction between the ^{14}N nuclei and the unpaired electron in the dilute solution. After preparation of RNP via the dialysis method, in contrast, the RNP signal became broader, indicating the location of nitroxide radicals in the hydrophobic solid core of RNP. As shown in Fig. S5, both RNPs have broad ESR spectra at pH values above 7.4, indicating the confinement of the TEMPO radicals in the solid core of RNP. With decreasing pH, the ESR signals of RNP^{pH} gradually change, and triplet signals are observed under acidic pH conditions, accompanying the

disintegration.   This observed signal change indicates the disintegration of RNP^{pH}.   In

contrast, no change in the ESR spectra of RNP^{Non-pH} was observed as a function of pH,

indicating that RNP^{Non-pH} possesses a core-shell type self-assembling structure

regardless of pH change.   When the ex vivo ESR assessment is utilized after

intravenous administration of RNP^{pH} to mice subjected to IR injury, the changes in ESR

spectra might be observed in renal ischemic lesion and we would verify the rational

strategy of ESEPT in vivo.   We administered the drugs (nitroxide radical

concentration :   75 mmol/kg) at 5 min after reperfusion and measured the ESR spectra

of the nitroxide radicals in plasma as a function of time.   The blood samples were

collected at 0.083, 0.25, 0.5, 3, 6 and 24 h after administration.   Fig. 5a-d shows the

time profile of drug concentration in blood.   Generally, nitroxide radicals are reduced

to hydroxylamine, which is not detected using ESR, by an in vivo reducing agent such

as ascorbic acid.   Since hydroxylamine also possesses radical scavenging capacity, the

total drug concentrations (nitroxide radicals + hydroxylamines) were determined by

adding potassium ferricyanide ($K_3[Fe(CN)_6]$) to re-oxidize hydroxylamines to nitroxide

radicals.   Contrary to the rapid clearance of low-molecular-weight 4-hydroxyl-TEMPO

and 4-amino-TEMPO from the bloodstream, the ESR signals of the both RNPs were

observed for a relatively long period of time.   The rapid clearance of

low-molecular-weight 4-amino-TEMPO and 4-hydroxy-TEMPO might be due to

preferential renal clearance and diffusion across the whole body. The insets in Fig.

5a-d show the ESR spectra of the oxidized samples after the additions of $K_3[Fe(CN)_6]$.

Low-molecular-weight TEMPO derivatives show a clear triplet signal, as shown in Fig.

5c-d. In contrast, the observed ESR signals of RNP^{pH} and RNP^{Non-pH} were broad

singlets in blood (see insets in Fig. 5a-b), suggesting that the TEMPO radicals are still

located in the solid core of the polymeric micelles in blood stream. The prevention of

renal elimination and the long blood circulation time of RNPs can be attributed to the

formation of polymeric micelles in blood. Next, ESR spectra in IR-kidneys were

measured. Fig. 5e-h shows the time profile of drug concentration in the injured renal

lesion. The signals of 4-hydroxyl-TEMPO and 4-amino-TEMPO completely

disappeared within 30 min and 6 h, respectively. In contrast, the signals of RNP^{pH} and

RNP^{Non-pH} were observed in the kidney for more than 6 h, as monitored by ESR

spectroscopy after re-oxidation by $K_3[Fe(CN)_6]$. This long retention of nitroxide

radicals in the kidney might be an important factor for the protection of renal function

after IR, because excess ROS gradually continues to be generated after reperfusion [21].

In addition, the administration of RNP^{pH} evoked the triplet ESR signal in the IR kidney,

whereas RNP^{Non-pH} did not show any change from the singlet spectra. This result

strongly suggests the disintegration of RNP^{pH} at the injured kidney lesion due to the lowered pH. Regardless of longest distribution of RNP^{Non-pH} in ischemic renal lesion, the site-specific disintegration of RNP^{pH} in the targeted organd would lead to the improved therapeutic effect on IR-AKI, as compared with RNP^{Non-pH}.

The side effects of nitroxide radicals

Moreover, we investigated the side effects of TEMPO derivatives because TEMPO derivatives are known to show severe side effects; e.g., dose-related antihypertensive action accompanied by reflex tachycardia, increased skin temperature, and seizures [22]. In particular, hypotensive action would be a serious adverse event during the treatment and surgery. The mean arterial blood pressure was measured at 15 min after the intravenous administration of the drugs. As shown in Fig. 6, 4-amino-TEMPO and 4-hydroxy-TEMPO drastically decreases in arterial blood pressure. In contrast, both RNPs inhibited the decrease in arterial blood pressure. There were no significant differences between the control, RNP^{pH} and RNP^{Non-pH} groups. Although the exact reason is still unknown, it is thought that the reduction of arterial blood pressure after administration of low-molecular-weight TEMPO derivatives is induced by an increase in endogenous nitric oxide (NO), resulting in vasodilatation *in*

vivo [23,24].   These results demonstrate that RNPs protect against blood pressure fluctuations because of the encapsulation of TEMPO moieties in hydrophobic core of RNP in the blood stream.

Discussion

Despite significant advances in medical treatments, AKI remains a major clinical problem associated with considerable morbidity and mortality, which has not decreased significantly over the last 50 years [25].   Although many promising drugs, in particular antioxidants, have been developed and shown to be of benefit in experimental models of AKI or renal IR injury, the results of recent clinical trials investigating these promising drugs have been largely negative.   For example, the use of native SOD has faced a number of problems ranging from its rapid proteolytic degradation, immunogenicity in vivo to prooxidant and cytotoxic activities at higher concentrations [26].   Although low-molecular-weight TEMPO derivatives also show therapeutic effect on renal IR injuries as previous reported [27], however, they are hard to utilize in clinic due to the side effects such as hypotensive action.   Additionally, their preferential renal clearance

inhibits long-term retainment of nitroxide radicals in injured renal lesion, resulting in lowered therapeutic effect.

Unlike the concept of existing drugs, the ESEPT can control the drug pharmacokinetics and the pharmaceutical activity due to the "on-off regulation" of nanoparticle in response to signal around target tissue area. We have to emphasize here that the nanoparticles possessing such signal switching characteristics tends to decrease their stability. Physical entrapment of low-molecular-weight drugs causes the leakage of the drug from the nanoparticle into the blood stream and would decrease in its therapeutic efficiency and cause severe side effects. Covalent conjugation of drug in hydrophobic segment of amphiphilic block copolymer, so called polymer drug, is one of the most important strategies to utilize "on-off" switching mechanism. As a result, the RNP^{pH} has the excellent therapeutic effect and prevents side effect for renal IR-AKI model in mice due to the strategy of ESEPT. We have revealed the disintegration of nanoparticle in injured kidney using the ESR spectroscopy, which is provide the evidence of the real therapeutic effect using the environment-sensitive specific disintegration of nanoparticles in vivo. Given their enhanced ability to scavenge ROS and reduce side effect by RNP^{pH}, the usage of RNP^{pH} might be a promising therapeutic strategy toward other oxidative stress injuries, regardless of renal IR-AKI. Moreover,

23

we believe that the strategy of ESEPT makes a contribution in clinical practice as a new type of nanomedicine.

Conclusion

This study demonstrates that the ESEPT strategy by pH-responsive RNP^{pH} improves the therapeutic efficiency and suppresses the significant side effects, using renal IR-AKI model in mice, due to the morphological change in nanoparticles within injured kidney area. This disintegration of RNP^{pH} in injured kidney area was confirmed by ESR spectra, which is evidence of real therapeutic effect using the environmental-sensitive disintegration of nanoparticle worked in vivo. Furthermore, the side effect of nitroxide radicals was markedly suppressed due to the compartmentalization of nitroxide radicals in the core of RNP^{pH} in untargeted area. From these results, the RNP^{pH} is promising as high performance nanomedicine toward oxidative stress injuries including renal IR-AKI.

Acknowledgements

Appendix. Supplementary data

Supplementary data related to this article can be found online.

References

[1] Star RA. Treatment of acute renal failure. Kidney Int 1998;54:1817–1831.

[2] Nath KA, Norby SM. Reactive oxygen species and acute renal failure. Am J Med

2000;109:665–678.

[3] Hirayama A, Nagase S, Ueda A, Oteki T, Takada K, Obara M, et al. In vivo imaging

of oxidative stress in ischemia-reperfusion renal injury using electron paramagnetic

resonance. Am J Physiol Renal Physiol 2005;288:F597–603.

[4] Nilakantan V, Hilton G, Maenpaa C, Van Why SK, Pieper GM, Johnson CP, et al.

Favorable balance of anti-oxidant/pro-oxidant systems and ablated oxidative stress

in Brown Norway rats in renal ischemia-reperfusion injury. Mol Cell Biochem

2007;304:1–11.

[5] Marchioli R, Schweiger C, Levantesi G, Tavazzi L, Valagussa F. Antioxidant

vitamins and prevention of cardiovascular disease: epidemiological and clinical trial

data. Lipids 2001;36Suppl:S53–S63.

[6] Davis ME, Chen ZG, Shin DM. Nanoparticle therapeutics: an emerging treatment

modality for cancer. Nat Rev Drug Discov 2008;7:771–782.

[7] Yokoyama M, Miyauchi M, Yamada N, Okano T, Sakurai Y, Kataoka K, et al.

Characterization and anticancer activity of the micelle-forming polymeric anticancer

drug adriamycin-conjugated poly(ethylene glycol)-poly(aspartic acid) block

copolymer. Cancer Res 1990;50:1693–1700.

[8] Kabanov AV, Chekhonin VP, Alakhov VYu, Batrakova EV, Lebedev AS, Melik-Nubarov NS, et al. The neuroleptic activity of haloperidol increases after its solubilization in surfactant micelles: Micelles as microcontainers for drug targeting. FEBS letters 1989;258:343–345.

[9] Matsumura Y, Maeda H. A new concept for macromolecular therapeutics in cancer chemotherapy: mechanism of tumoritropic accumulation of proteins and the antitumor agent smancs. Cancer Res 1986;46:6387–6392.

[10] Yamamoto Y, Nagasaki Y, Kato Y, Sugiyama Y, Kataoka K. Long-circulating poly(ethylene glycol)-poly(D,L-lactide) block copolymer micelles with modulated surface charge. J Controlled Release 2001;77:27–38.

[11] Nishiyama N, Okazaki S, Cabral H, Miyamoto M, Kato Y, Sugiyama Y, Nishio K, Matsumura Y, Kataoka K. Novel cisplatin-incorporated polymeric micelles can eradicate solid tumors in mice. Cancer Res. 2003;63:8977–8983.

[12] Kirpotin DB, Drummond DC, Shao Y, Shalaby MR, Hong K, Nielsen UB, et al. Antibody targeting of long-circulating lipidic nanoparticles does not increase tumor localization but does increase internalization in animal models. Cancer Res 2006;66:6732–6740.

[13] Emoto K, Nagasaki Y, Kataoka K. A Core-Shell Structured Hydrogel Thin Layer

on Surfaces by Lamination of a Poly(ethylene glycol)-*b*-poly(D,L-lactide) Micelle

and Polyallylamine. Langmuir 2000;16: 5738–5742.

[14] Bae Y, Nishiyama N, Fukushima S, Koyama H, Yasuhiro M, Kataoka K.

Preparation and biological characterization of polymeric micelle drug carriers with

intracellular pH-triggered drug release property: tumor permeability, controlled

subcellular drug distribution, and enhanced in vivo antitumor efficacy.

Bioconjugate Chem 2005;16:122–130.

[15] Yoshitomi T, Miyamoto D, Nagasaki Y. Design of core-shell-type nanoparticles

carrying stable radicals in the core. Biomacromolecules 2009;10:596–601.

[16] Yoshitomi T, Suzuki R, Mamiya T, Matsui H, Hirayama A, Nagasaki Y.

pH-sensitive radical-containing-nanoparticle (RNP) for the L-band-EPR imaging

of low pH circumstances. Bioconjugate Chem 2009;20:1792–1798.

[17] Marushima A, Suzuki K, Nagasaki Y, Yoshitomi T, Toh K, Tsurushima H, et al.

Newly Synthesized Radical-Containing Nanoparticles (RNP) Enhance

Neuroprotection After Cerebral Ischemia-Reperfusion Injury. Neurosurgery

2011;68:1418–1426.

[18] Soule BP, Hyodo F, Matsumoto K, Simone NL, Cook JA, Krishna MC, et al. The

chemistry and biology of nitroxide compounds. Free Radic Biol Med 2007;42:1632–1650.

[19] Krishna MC, Russo A, Mitchell JB, Goldstein S, Dafni H, Samuni A. Do nitroxide antioxidants act as scavengers of O2-. or as SOD mimics? J Biol Chem 1996;271:26026–26031.

[20] Prathapasinghe G, Siow Y, Xu Z, O K. Inhibition of cystathionine-beta-synthase activity during renal ischemia-reperfusion: role of pH and nitric oxide. Am J Physiol Renal Physiol 2008;295:F912–F922.

[21] Kim J, Jung K, Park K. Reactive oxygen species differently regulate renal tubular epithelial and interstitial cell proliferation after ischemia and reperfusion injury. Am J Physiol Renal Physiol 2010; 298: F1118–F1129.

[22] Hahn SM, Sullivan FJ, DeLuca AM, Bacher JD, Liebmann J, Krishna MC, et al. Hemodynamic effect of the nitroxide superoxide dismutase mimics. Free Radic Biol Med 1999;27:529–535.

[23] Patel K, Chen Y, Dennehy K, Blau J, Connors S, Mendonca M, et al. Acute antihypertensive action of nitroxides in the spontaneously hypertensive rat. Am J Physiol. Regul Integr Comp Physiol 2006;290:R37–R43.

[24] Wilcox C, Pearlman A. Chemistry and antihypertensive effects of tempol and other

nitroxides. Pharmacol Rev 2008;60:418–469.

[25] Sheridan A, Bonventre J. Cell biology and molecular mechanisms of injury in ischemic acute renal failure. Curr Opin Nephrol Hypertens 2000;9:427-434.

[26] Nelson SK, Bose SK, McCord JM. The toxicity of high-dose superoxide-dismutase suggests that superoxide can both initiate and terminate lipid-peroxidation in the reperfused heart. Free Radic Biol Med 1994;16:195–200.

[27] Chatterjee PK, Cuzzocrea S, Brown PA, Zacharowski K, Stewart KN, Mota-Filipe H, et al. Tempol, a membrane-permeable radical scavenger, reduces oxidant stress-mediated renal dysfunction and injury in the rat. Kidney Int 2000;58:658–673.

Figure Legends:

Figure 1. Schematic illustration of "Environmental-Signal-Enhanced Polymer Drug Therapy (ESEPT)"

Figure 2. In vitro characterization of RNP^{pH} and RNP^{Non-pH} (**a**) Size distributions of RNP^{pH} (red line) and RNP^{Non-pH} (blue line) (**b**) Effect of pH on the light scattering intensities of RNP^{pH} (red circle) and RNP^{Non-pH} (blue circle). The normalized scattering intensity (%) is expressed as the value relative to that at pH 8.2 (**c**) Superoxide scavenging activities of RNP^{pH} and RNP^{Non-pH} using a spin trapping agent at pH 6.0 and 7.4. (The bar graphs represent means ± SE for 3 independent experiments. *P <0.05, Student's t-test)

Figure 3. Therapeutic effect of RNP on IR-AKI. (a) BUN and (b) Cr in plasma of mice at 24 h after reperfusion following 50min ischemia. Sham veh, sham-operated and vehicle-treated group; IR veh, vehicle treated group; IR RNP(pH), RNP^{pH}-treated group; IR RNP(non-pH), RNP^{Non-pH}-treated group; IR AT, 4-amino-TEMPO treated group; IR HT, 4-hydroxy-TEMPO treated group. (Values expressed as mean ± SE. * P < 0.0001 as compared to IR veh. ** P < 0.005 as compared to IR veh. *** P < 0.05 as

compared to IR veh. n = 7, ANOVA) **(c)** Representative photomicrographs (hematoxylin and eosin staining, magnification ×200) of renal cortex of the kidneys in mice at 24 h after reperfusion following 50 min ischemia.   Sham/vehicle, sham-operated and vehicle-treated group; IR/vehicle, vehicle treated group; IR/RNP^{pH}, RNP^{pH}-treated group; IR/RNP^{Non-pH}, RNP^{Non-pH}-treated group; IR/AT, 4-amino-TEMPO treated group; IR/HT, 4-hydroxy-TEMPO treated group.

Figure 4.   Suppressive effect on the generation of superoxide anion, inflammation cytockine and lipid oxidation.   Sham veh, sham-operated and vehicle-treated group; IR veh, vehicle treated group; IR RNP(pH), RNP^{pH}-treated group; IR RNP(non-pH), RNP^{Non-pH}-treated group; IR AT, 4-amino-TEMPO treated group; IR HT, 4-hydroxy-TEMPO treated group. (a) Superoxide in renal tissue homogenate was measured by dihydroethidium (DHE). Superoxide values were expressed as the value related to fluorescent intensity of sham veh group.   (Values expressed as mean ± SE. * $P < 0.05$ as compared to IR veh. n = 5, ANOVA) (b) DHE staining in kidneys subjected to I/R injury. Mice were subjected to 50 min of renal ischemia or sham-operation, then harvested 24 h after reperfusion. The kidney sections were stained using the DHE.   (c) Measurement of thiobarbituric acid-reactive substances (TBARS) in the kidneys of

mice subjected to 50 min ischemia-reperfusion. (Values expressed as mean ± SE. * $P <$ 0.05 as compared to IR veh. [#] $P < 0.001$ as compared to RNP^{pH}. n = 5, ANOVA)

(d) Measurement of IL-6 in the plasma of mice subjected to 50 min ischemia-reperfusion. (Values expressed as mean ± SE. * $P < 0.05$ as compared to IR veh. n = 5, ANOVA)

Figure 5. **Time profile of drug concentration in (a-d) blood and (e-h) injured kidney.** All drugs were injected from tail vein of mice subjected to 50 min ischemia at 5 min after reperfusion. Signal intensities after adding potassium ferricyanide ($K_3[Fe(CN)_6]$) to re-oxidize hydroxylamines to nitroxide radicals mean the total drug concentrations (nitroxide radicals + hydroxylamines) (Inset) the ESR spectra of the oxidized samples (15 min after reperfusion) by the additions of $K_3[Fe(CN)_6]$. The intravenous dose was 75 μmol/kg of nitroxide concentration in all drugs to mice. (mean ± SE, n = 5 per group).

Figure 6. **The change in blood pressure at 15 min after the administration of drugs** Mean arterial pressures were measured at 15 min after bolus injection of RNP^{pH}, RNP^{Non-pH}, 4-amino-TEMPO (AT) and 4-hydroxy-TEMPO (HT) in ICR mice. TEMPO

33

concentration of all substances was 75 μmol/kg.   (Values expressed as mean ± SE. * P

< 0.05 as compared to PBS. n = 5, ANOVA)

Table Legend:

Table 1 Effect of RNP^{pH}, RNP^{Non-pH}, amino-TEMPO and treatment on morphological

changes as assessed by histopathological examination of kidneys of the mice subjected

to 50 min ischemia-reperfusion.

Figure1.

"Environmental-Signal-Enhanced Polymer Drug Therapy (ESEPT)"
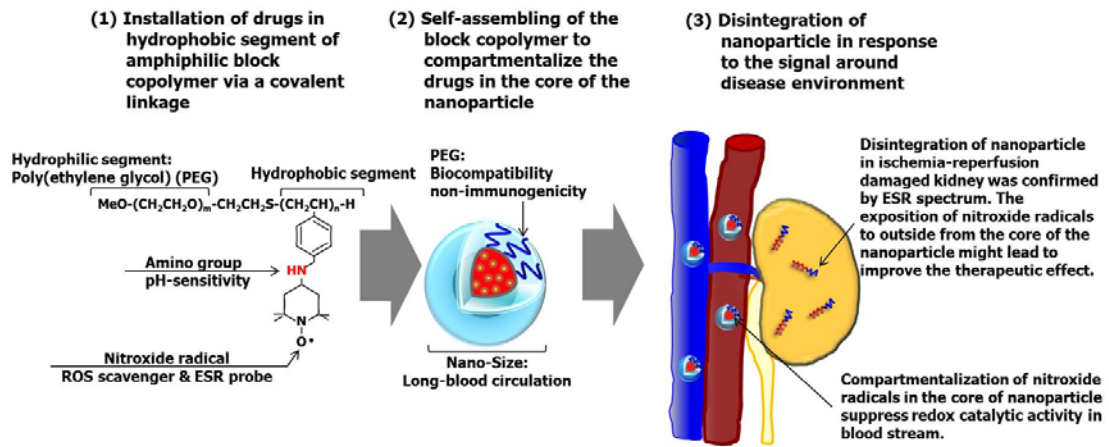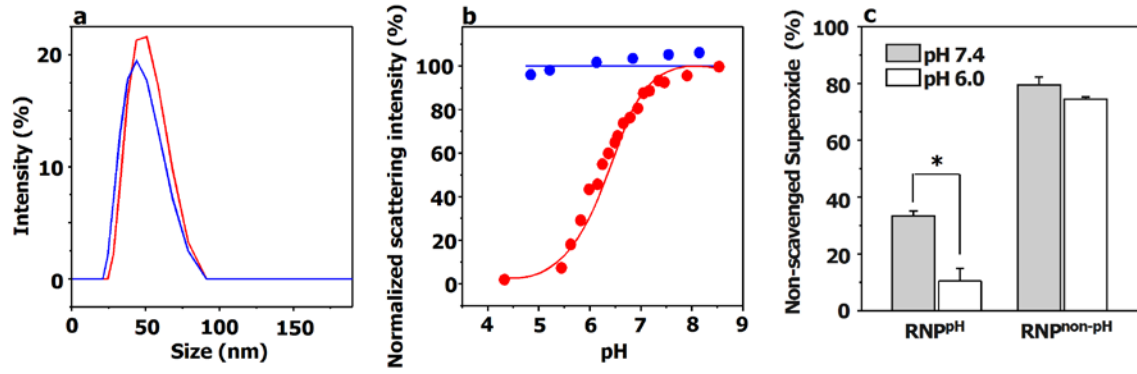
Figure2.

Figure 3.
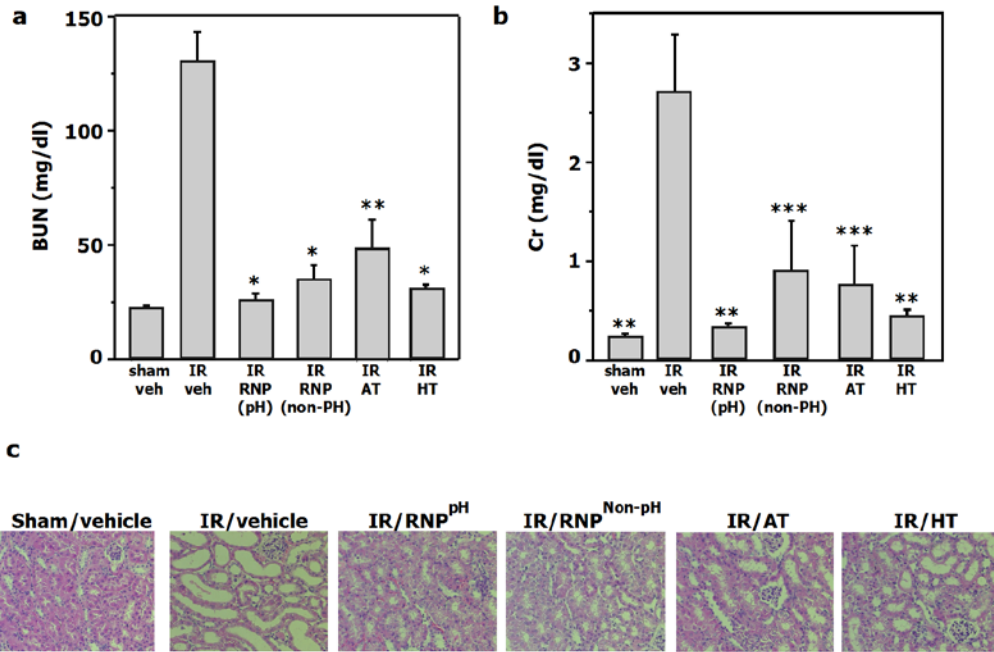
Figure 4.
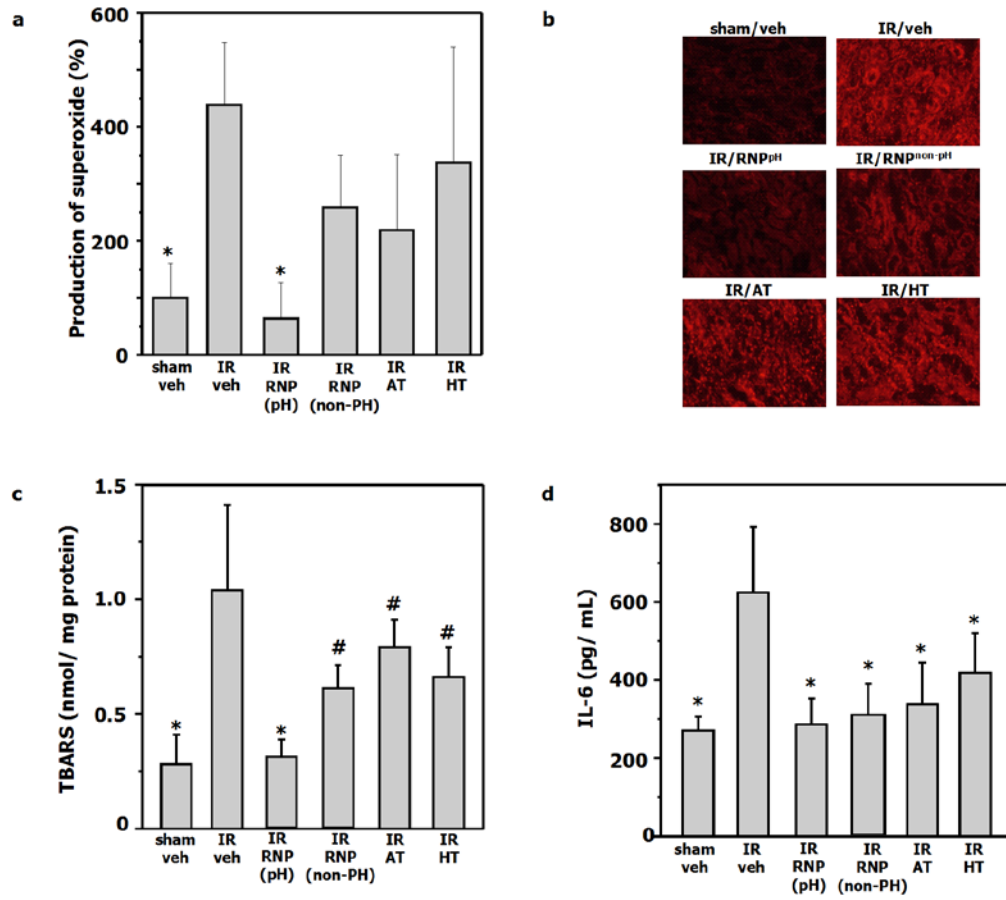
Figure 5.
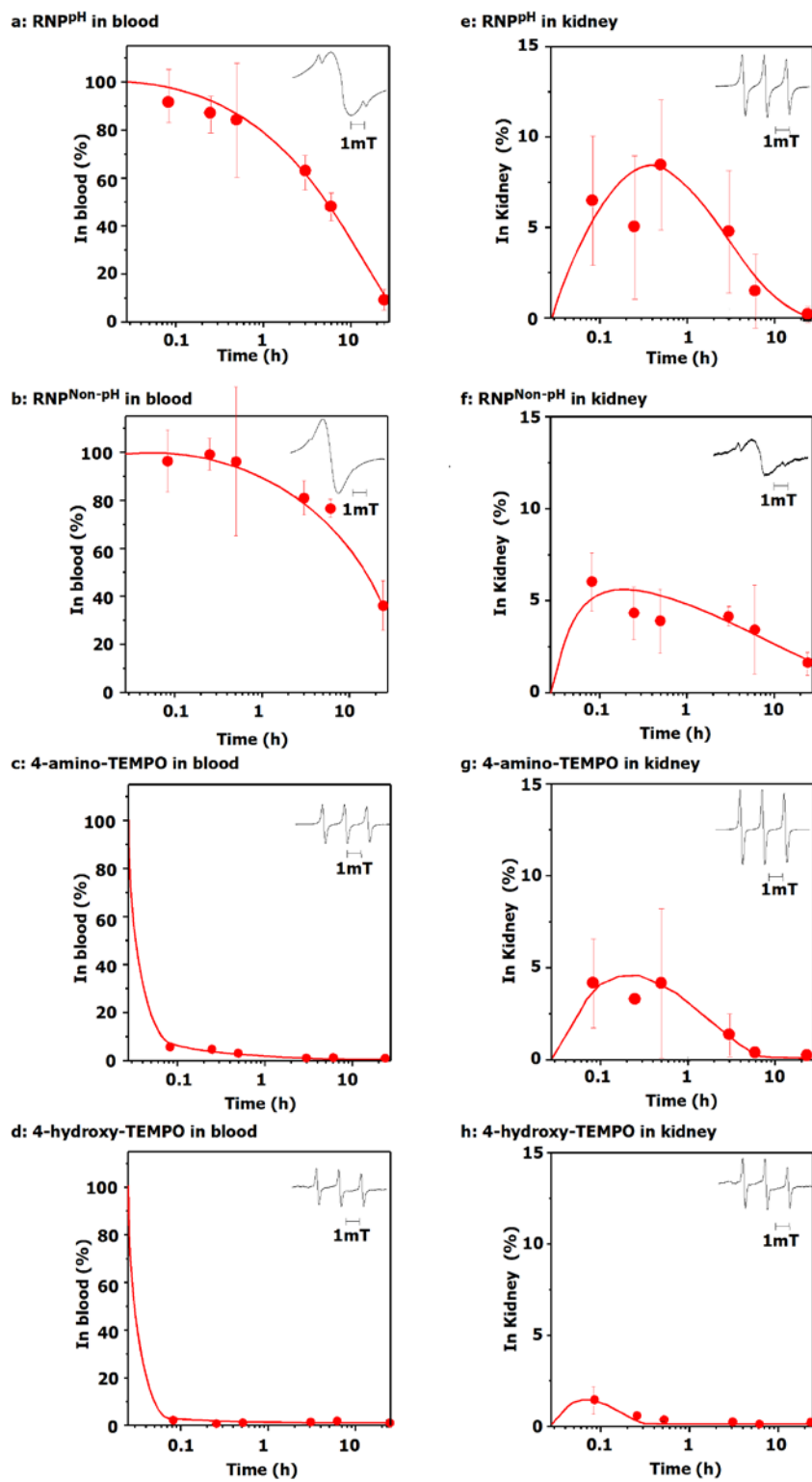
Figure 6.
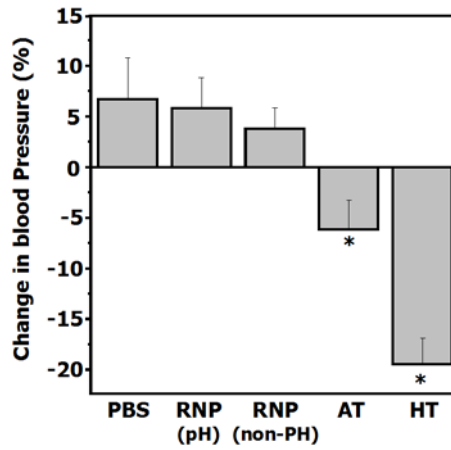
Table 1

Group	Tubular cell swelling	Interstitial edema	Tubular dilatation
sham vehicle	-	-	-
IR vehicle	+++	+++	+++
IR RNP^{pH}	-	-	-
IR RNP^{non-pH}	+	+	+
IR amino-TEMPO	++	++	++
IR hydroxy-TEMPO	++	++	++

The ROS scavenging and renal protective effects of pH-responsive nitroxide radical-containing nanoparticles

Toru Yoshitomi[a], Aki Hirayama[b] and Yukio Nagasaki[a,c,d,]

[a] Graduate School of Pure and Applied Sciences, University of Tsukuba, Tennoudai 1-1-1, Tsukuba, Ibaraki, 305-8573, Japan
[b] Center for Integrative Medicine, Tsukuba University of Technology, Kasuga 4-12-7, Tsukuba, 305-8521, Ibaraki, Japan
[c] Master's School of Medical Sciences, Graduate School of Comprehensive Human Sciences, University of Tsukuba, Tennoudai 1-1-1, Tsukuba, Ibaraki, 305-8573, Japan
[d] Satellite Laboratory, International Center for Materials Nanoarchitectonics (MANA), National Institute for Materials Science (NIMS), Tennoudai 1-1-1, Tsukuba, Ibaraki, 305-8573, Japan

Methods:

Preparation of RNP^{pH} by dialysis method

90 mg of MeO-PEG-b-PMNT were dissolved in 10 mL of DMF, and the polymer solution was transferred into a membrane tube (Spectra/Por, molecular-weight cutoff size: 3,500, Spectrum, USA) and then dialyzed for 24 h against 2 L of water, which was changed after 2, 5, 8 and 20 h. The RNP^{Non-pH} was prepared from PEG-b-PMOT by the dialysis method, similar to RNP^{pH}.

Preparation of non-pH-responsive nitroxide radical-containing-particle (RNP^{Non-pH})

Non-pH-responsive RNP^{Non-pH} was prepared by a self-assembling amphiphilic block copolymer (PEG-b-PMOT) composed of the PEG segment and the PMS segment possessing TEMPO moieties as a side chain via ether linkage, as show in Fig. S1. Briefly, after 200 mg (25 μmol) of the MeO-PEG-b-PCMS (Mn = 8,300) were weighed into a 10-mL flask, a DMF (1 mL) was added, then DMF (1 mL) involved 4-hydroxy-TEMPO (260 mg, 1.25 mmol) and sodium hydride (70.3 mg, 2.5 mmol) was added to the flask and stirred for 5 h at room temperature. The reacted polymer was filtrated and recovered by precipitation into 10 mL of cold 2-propanol (-15 °C) and centrifugation for 30 min at 5,000 rpm (4,500 g). In order to purify the obtained polymer, the precipitation-centrifugation cycle was repeated three times, followed by freeze-drying with benzene. The yield of the obtained PEG-b-PMOT copolymer was 70.0 % (184 mg).

Dynamic light scattering (DLS) experiments and X-band electron spin resonance (ESR) experiments as a function of pH

The light scattering intensities of the pH-sensitive RNP were measured as a function of pH using a light scattering spectrometer (Nano ZS, ZEN3600, Malvern Instruments, Ltd., UK) equipped with a He-Ne laser that produces vertically polarized incident beams at a detection angle of 173° at 25 °C. Briefly, 3.5 mg/mL of the RNP solution was prepared as stock solution **A** after the formation of the RNPs by the dialysis method. Britton-Robinson buffers (100 μL each) with various pH values, which

were prepared from a stock solution containing 1M phosphoric acid, 1M boric acid and 1M acetic acid and by adjusting the pH value with NaOH, were added to stock solution **A** (400 μL). The mixtures with various pH values were transferred to the cells immediately, followed by DLS measurement. The ESR measurements were carried out under the following conditions: frequency, 9.4190 GHz; power, 8.00 mW; field, 333.8 ± 50 mT; sweep time, 2.0 min; modulation, 0.1 mT; time constant, 0.1 s.

Morphological studies

The kidneys were fixed in a 10 % neutral buffered formalin solution and embedded in paraffin for use in histopathological examination. Thick sections (4 μm) were cut, deparaffinized, hydrated and HE stained. The renal sections were examined in a blind fashion for tubular cell swelling, interstitial edema, and tubular dilatation in all treatments. Each kidney slide was examined and assigned according to the severity of changes using scores on a scale of none (-), mild (+), moderate (++), and severe (+++) damage.
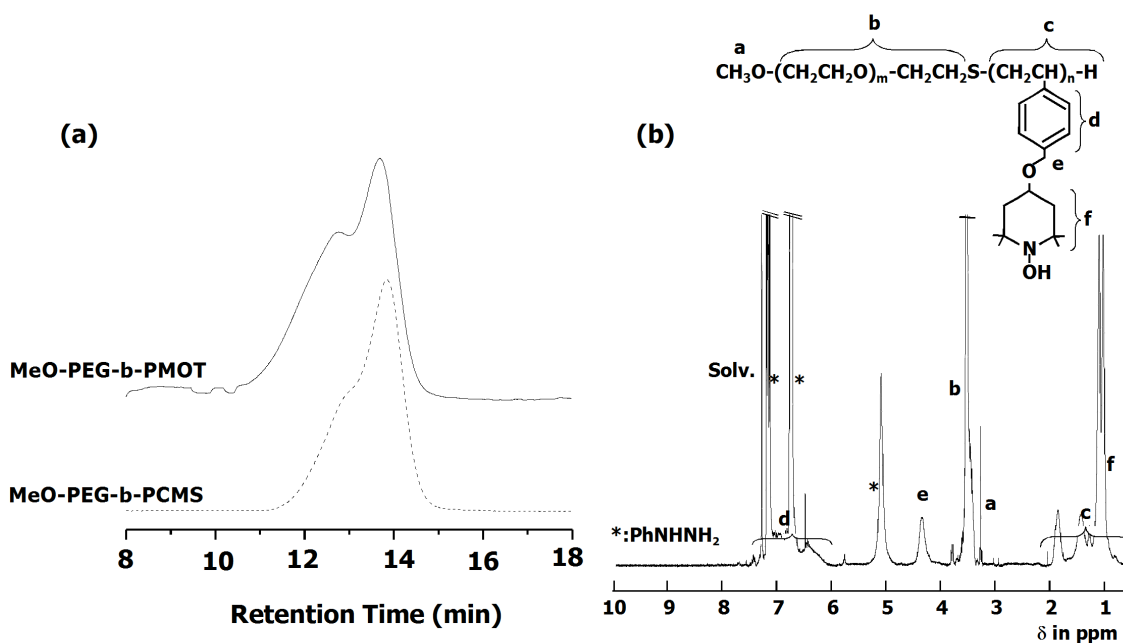

Figure S1. (a) SEC diagram and (b) ^{1}H NMR spectrum of MeO-PEG-*b*-PCMS and MeO-PEG-*b*-PMOT in the presence of phenylhydrazine. (SEC apparatus, TOSOH HLC-8120GPC; detector, RI; column, TOSOH SUPER HZ4000+3000; solvent, THF (containing 2 w% triethylamine); flow rate, 0.35 mL/min; calibration, standard PEGs.)

2

A. DMPO+RNP^{Non-pH}

B. RNP^{Non-pH}

A-B

H

Without RNP^{Non-pH}

H₀

330   332   334   336

Field (mT)

amount of superoxide (%) = H/H₀ × 100
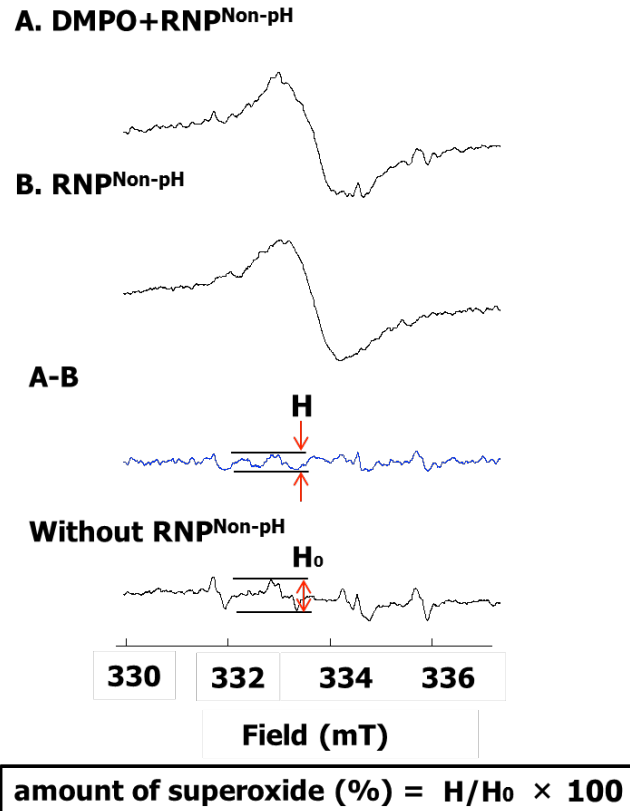
**Figure S2.** ESR spectrum of the RNP^{non-pH} and DMPO at pH 6.0 and equation of amount of superoxide in the present of RNP^{non-pH}.
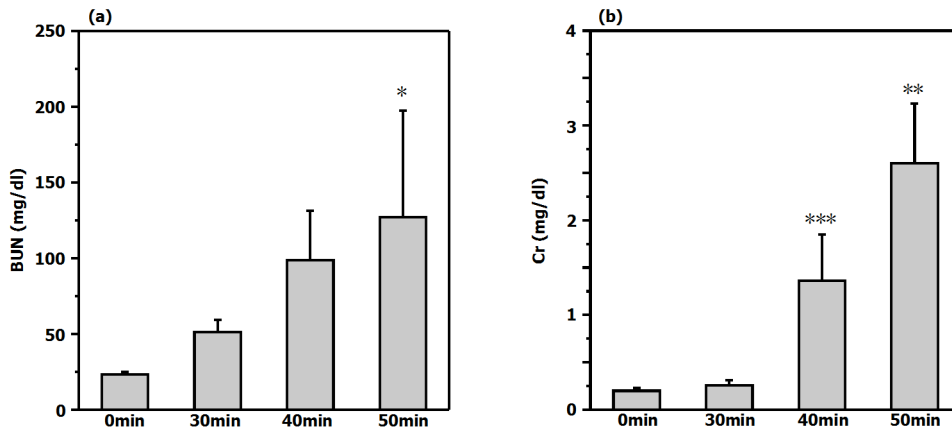
Figure S3. The ischemic time-dependent change of plasma blood urea nitrogen (BUN) and plasma creatinine (Cr) on acute kidney injury induced by ischemia-repefusion. (Values expressed as mean ± SE. * $P < 0.0001$ as compared to 0 min. ** $P < 0.01$ as compared to 0 min. *** $P < 0.05$ as compared to 0 min. n = 5, ANOVA)
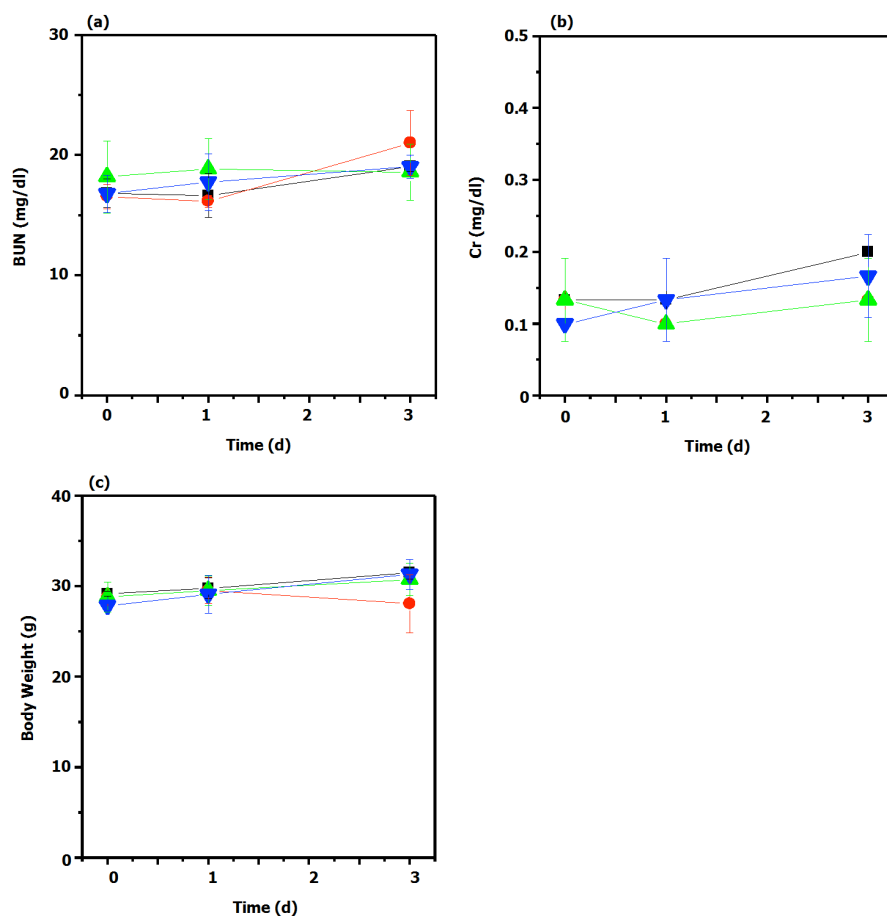
Figure S4. Time course of plasma blood urea nitrogen (BUN), plasma creatinine (Cr) and body weight of normal mice after intravenous administration of PBS (black square), 4-amino-TEMPO (red circle), RNP^{pH} (green triangle) and RNP^{Non-pH} (blue triangle).
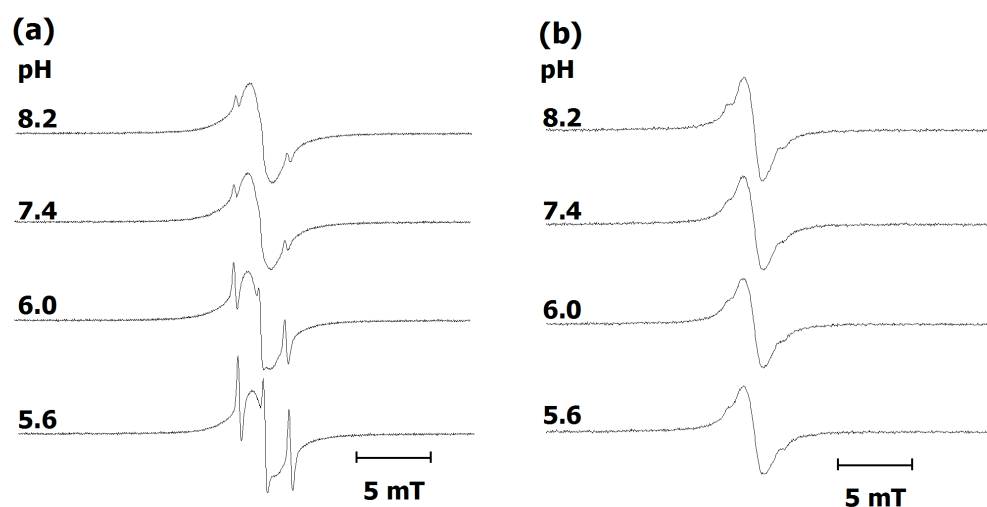
Figure S5. X-band ESR spectra of the RNP^{pH} (a) and RNP^{Non-pH} (b) as a function of pH, at pH 5.6, 6.0, 7.4 and 8.2, in Britton-Robinson buffer prepared from a stock solution containing 1 M phosphoric acid, 1 M boric acid and 1 M acetic acid, and by adjusting the pH value with NaOH.

Table S1   Total dose of administration and TEMPO concentrations into all drugs

	RNP^{pH}	RNP^{non-pH}	AT	HT	vehicle (PBS)
Conc. (mg/kg)	3	1.5	0.4	0.4	0
TEMPO conc. (μmol/kg)	2.5	2.5	2.5	2.5	0